

Nancy A. Marley* and Jeffrey S. Gaffney
Argonne National Laboratory, Argonne, Illinois

1. INTRODUCTION

Gaseous ammonia is the third most abundant nitrogen compound and the most abundant alkaline trace gas in the atmosphere. As the principal neutralizing agent for atmospheric acids, ammonia plays an important role in aerosol formation. It is thought to be a major influence on regional air quality, atmospheric visibility, and acid deposition. Although the main source of atmospheric ammonia is agriculture, other sources include industries, landfills, household products, biomass burning, motor vehicles, and wild animals (Sutton et al., 2000).

The main sink for ammonia in the atmosphere is the heterogeneous reaction with sulfuric acid, yielding ammonium sulfate $[(\text{NH}_4)_2\text{SO}_4]$ and ammonium bisulfate $[\text{NH}_4\text{HSO}_4]$ salts. Reactions with nitric and hydrochloric acids form ammonium nitrate (NH_4NO_3) and ammonium chloride (NH_4Cl) salts. These NH_4^+ aerosols affect Earth's radiative balance, both directly by scattering incoming radiation and indirectly by acting as cloud condensation nuclei. They also contribute to the long-range transport of acidic pollutants, because the atmospheric lifetime of ammonia is short (<24 h), while that of NH_4^+ salts is on the order of a few days (Adams et al., 1999). Long-range transport can result in deposition of the NH_4^+ salts far from the emission sources. After deposition, NH_4^+ aerosols can contribute to soil acidification, forest decline, and eutrophication of waterways (Asman, 1994; Aneja et al., 1998).

Approximately 54 Tg of ammonia nitrogen are emitted globally each year, with the largest portion (~41%) coming from the excreta of domestic animals (Bouwman et al., 1997; Schlesinger and Hartley, 1992). Recent studies have suggested that ammonia emissions from motor vehicle traffic might be the most important source in urban areas (Fraser and Cass, 1998; Moeckli et al., 1996; Sutton et al., 2000). Vehicles equipped with catalytic converters and operating under fuel-rich conditions generate ammonia by reaction of NO and H within the converter. Estimated emission factors of ammonia from motor

vehicles have increased from 1.3 mg/km in 1981 (Pierson and Brachaczek, 1983) to about 60 mg/km in 1993 (Fraser and Cass, 1998), in line with an increase of vehicles equipped with three-way catalytic converters from <10% in 1981 to >75% in 1993.

Accelerated growth and high population densities in megacities result in rapid deterioration of air quality, with high loadings of both fine primary aerosols and trace gases that can lead to the formation of secondary aerosols. Megacities function as large sources of atmospheric aerosols, which — after transport — can influence air quality and climate on urban, regional, and global scales. The magnitude and even the sign of the radiative impacts of the transported aerosols depend on their chemical compositions and sizes, as well as their spatial distributions in the atmosphere.

The Mexico City metropolitan area, which occupies approximately 1300 km² and has a population of about 18 million, is one of the largest megacities in the world and is well known for its high levels of air pollution and visibility reduction. Emissions from the Mexico City basin are estimated to contribute 15 megatons of fine aerosol (PM-2.5) per year to the surrounding regions (Gaffney et al., 1999). This fine aerosol is composed of 32% organic carbon, 15% elemental carbon, 10% ammonium nitrate, and 20% ammonium sulfate (Chow et al., 2002). The emissions of sulfate aerosols alone from the MCMA are estimated at 1% of the total global burden (Barth and Church, 1999).

In April of 2003, as part of the Mexico City Metropolitan Area (MCMA) 2003 air quality study, we obtained measurements of ammonia at the National Center for Environmental Research and Training (Centro Nacional de Investigación y Capacitación Ambiental, or CENICA), on the Iztapalapa campus of the Universidad Autónoma Metropolitana (UAM). Measurements were obtained continuously, over an open path of 244 m, with a near-infrared tunable diode laser (NIRTDL) system equipped with a telescope and retro-reflector. Fifteen-minute averages of the data clearly showed significant levels of ammonia in the Mexico City air, with evidence of aerosol formation during periods of high photochemical activity. The advantages of the NIRTDL system for the study of both aerosol formation and gas to particle formation is discussed, and the data obtained in the Mexico City megacity are presented.

*Corresponding author address: Nancy A. Marley, Environmental Research Division, Argonne National Laboratory, Argonne, IL 60439-4843; e-mail: marley@anl.gov.

2. INSTRUMENTAL DESIGN

Denuder techniques (Ferm, 1979) employing coatings that capture ammonia and enable sensitive, artifact-free measurements have been used for many years to determine ammonia in the atmosphere. However, these methods are labor intensive and time consuming, and they require long sample collection times. In addition, the longer sampling times needed for measurements at low concentrations than at higher levels result in varying time resolutions when atmospheric concentrations fluctuate widely.

More recently, other methods have been employed to achieve continuous measurements of atmospheric ammonia. These include continuous-flow denuders, coupled with conductivity detection; catalytic conversion to NO, followed by chemiluminescence detection; photofragmentation to NH, followed by detection with laser-induced fluorescence; photoacoustic spectroscopy; and chemical ionization mass spectrometry (Fehsenfeld et al., 2002). All of these techniques require pumping the sample into an instrument for analysis. Because ammonia forms strong hydrogen bonds with water, it tends to be deposited on the surfaces of materials exposed to air. The result can be sample losses, high backgrounds, and memory effects due to the deposition and subsequent release of ammonia on sample tubing and instrument walls.

Open-path, in-situ measurement techniques avoid the problems associated with wall losses and memory effects. In addition, they enable the continuous, real-time measurements of gas-phase species that are necessary to study aerosol formation and deposition rates. The high spectral resolution and tunability of diode lasers permit open-path measurements of components in a complex mixture. These systems are capable of rapid time response, operate near room temperature, and are relatively inexpensive and compact, making them attractive for field applications.

The instrument used in these studies is a NIRTDL system designed for in-situ, noninvasive measurements of ammonia in ambient air (LasIR, Unisearch Associates, Inc.). The system uses a GaAs diode laser, which emits radiation at 0.7-2.7 μm . The laser can be tuned to a single rotational-vibrational line of ammonia by varying the temperature and the current applied. A thermoelectric cooler, in conjunction with an active servo loop, maintains the diode temperature close to the set point. This provides unequivocal identification with a very high degree of discrimination against interfering species. High-frequency modulation techniques are used to yield sensitivities in the range of ppbv-m (parts per billion by volume-meter).

The system, shown schematically in Figure 1, consists of two major components: (1) the control module, containing the electronics and reference cell, and (2) the optics, which consists of a telescope, a retro-reflector, and a fiber optic transmission cable.

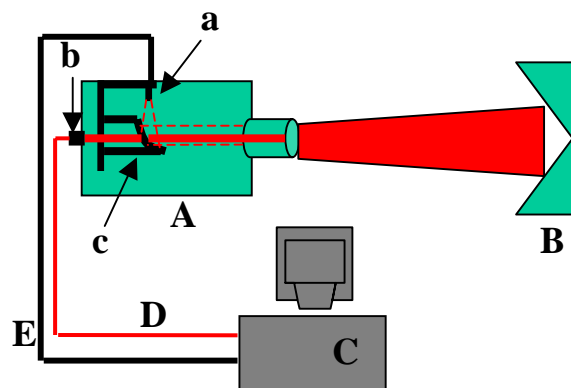


Figure 1. Schematic representation of the NIRTDL system, including telescope (A), detector (a), collimating lens (b), off-axis parabolic mirror (c), retro-reflector (B), control module (C), fiber optic cable (D), and coaxial cable (E).

The telescope, shown in Figure 2, launches the diode laser beam across an open path to the retro-reflector. The laser beam is delivered to the telescope by a fiber optic cable coupled to an aspheric lens. A slightly diverging beam is launched through the center of an off-axis parabolic mirror (OAP). The divergence of the beam is adjusted to the size needed to fill the retro-reflector mirror array (Figure 3) at the end of the measurement path. The OAP focuses the returning light from the retro-reflector array onto an infrared detector inside the telescope. The voltage signal from the detector is transmitted to the control module by means of a coaxial cable.

The control module (Figure 4) houses the diode laser, as well as a reference cell and a calibration cell that both contain ammonia gas. The diode laser beam is coupled to a fiber optic cable, which in turn is coupled to a fiber optic beam splitter where the beam is divided into two outputs (90:10). The 10% output passes through a 13-cm sealed reference cell that locks the laser wavelength onto the absorption feature. The 90% output can be directed either through a 13-cm sealed calibration cell containing ammonia gas at 661 ppmv or through the output fiber optic to the telescope.



Figure 2. Telescope assembly used to launch the diode laser beam.



Figure 3. Retro-reflector assembly used to return the divergent diode laser beam to the telescope.



Figure 4. Control module showing internal reference (lower) and calibration (upper) cells.

As the laser is scanned across the absorption feature, an increase in laser power results in a sloping background (Figure 5). To remove this background, the diode laser is frequency modulated, and phase-sensitive detection is used to detect the absorption feature. This method also discriminates against features that do not exhibit wavelength-dependent changes.



Figure 5. Normal absorption feature (A); first harmonic, $1f$ (B); and second harmonic, $2f$ (C).

The transmitted laser intensity can be expressed as a cosine Fourier series with coefficients given by the following equation:

$$H_n(\nu_L) = \frac{2}{\pi} \int I_0(\nu_L + m\gamma \cos\theta) \exp[-\sigma(\nu_L + m\gamma \cos\theta)nL] \cos n\theta d\theta, \quad (1)$$

where I_0 is the laser intensity, ν_L is the laser frequency, $\theta = \omega t$ is the modulation frequency, $m = \delta\nu/\gamma$ is the modulation coefficient, and γ is the half width at half maximum (HWHM) of the absorption line. Detection at the first harmonic ($n = 1$ or $1f$) gives a first-derivative line shape. Second-harmonic detection ($n = 2$ or $2f$) gives a second-derivative line shape. The latter is more commonly used, as it removes the sloping background most efficiently without a large reduction in signal. It also discriminates against features that do not exhibit wavelength-dependent changes.

3. MEXICO CITY MEASUREMENTS

The telescope launching element was placed on the roof of the CENICA building on the UAM campus. The retro-reflector was placed on the roof of an adjacent teaching building, 122 m from the telescope, resulting in a total open-path length of 244 m. Detection limits for ammonia with this system have been estimated at 0.203 ppm-m, with a signal:noise ratio of 1 in the 1-Hz band width (Table 1). This estimate gives a detection limit of approximately 0.8 ppb for a path length of 244 m.

Table 1. Estimated detection limits and line characteristics for measurement of ammonia gas with the NIRTDL system (Martin, 2002).

| Parameter | Unit | Value |
|-----------------|---------------------------|-------------------------|
| Wave number | cm ⁻¹ | 6478 |
| Wavelength | μm | 1.544 |
| Line strength | cm-molecule ⁻¹ | 3.7 x 10 ⁻²² |
| Line width | cm ⁻¹ | 0.060 |
| Detection limit | ppm-m | 0.203 |

Some of the data obtained at this site are shown in Figure 6. Daily maximum values during this period were 40-110 ppb. Ammonia values reached a maximum before noon on each day and fell rapidly just before midday, indicating ammonium aerosol formation in the afternoon.

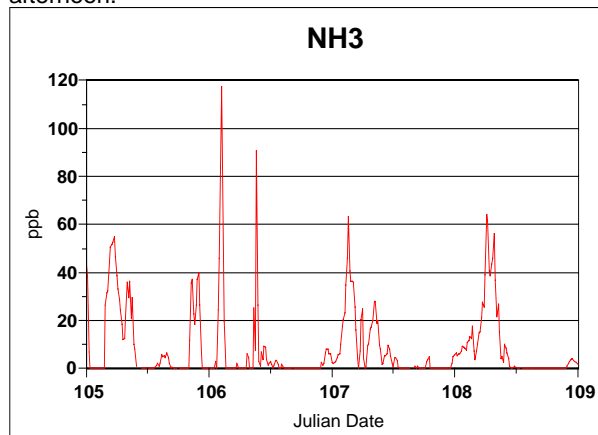


Figure 6. Ammonia measurements obtained in Mexico City on April 15-19, 2003.

Particle light scattering measurements (b_{sp}) were obtained at the same site with an integrating nephelometer. Results for the same time period are shown in Figure 7. These measurements confirm the formation of scattering particles in the early afternoon as the ammonia levels begin to fall.

4. CONCLUSIONS

This work demonstrates the use of the NIRTDL system for the measurement of ammonia gas in-situ. The open-path system avoids problems with losses and memory effects often encountered with ammonia measurements. In addition, the system yields the continuous, near-real-time measurements of gas-phase ammonia that are needed to study aerosol formation and deposition rates in urban areas. The high spectral resolution and tunability of the diode laser provide unequivocal identification with a very high degree of

discrimination against interfering species, while frequency modulation techniques yield sensitivities in the range of ppbv-m.

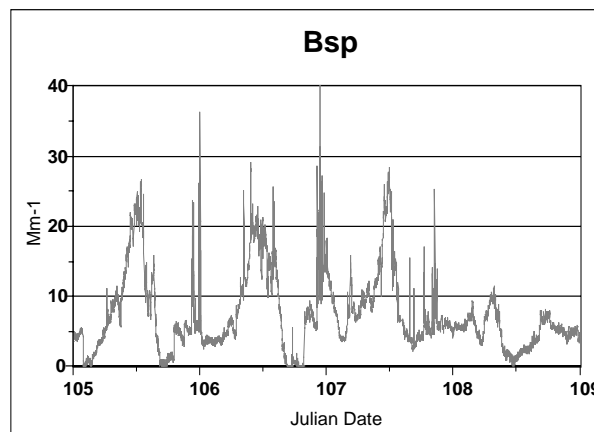


Figure 7. Particle light scattering (b_{sp}) in Mexico City on April 15-19, 2003.

5. ACKNOWLEDGMENTS

This effort was supported by the U. S. Department of Energy (USDOE), Office of Science, Office of Biological and Environmental Research, Atmospheric Chemistry Program, under contract W-31-109-Eng-38. We thank Mr. Peter Lunn (USDOE) for his continuing encouragement.

We also thank Drs. Luisa and Mario Molina of the Massachusetts Institute of Technology for their leadership and untiring help with the work in Mexico City. Acknowledgements, as well, go to the entire group of Mexican and U.S. scientists who were part of the MCMA 2003 field study and to the staff of CENICA for allowing us to set up our equipment at their facility.

6. REFERENCES

- Adams, P.J., J.H. Sienfeld, and D. Koch, 1999: Global concentrations of tropospheric sulfate, nitrate, and ammonium aerosol simulated in a general circulation model. *J. Geophys. Res.*, **104**, 13,791-13,823.
- Aneja, V.P., G.C. Murray, and J. Southerland, 1998: Atmospheric nitrogen compounds: Emissions, transport, transformation, deposition and assessment. *EM*, 22-25.
- Asman, W.A., 1994: Emission and deposition of ammonia and ammonium. *Nova Acta Leopold*, **70**, 263-297.
- Barth, M.C., and A.T. Church, 1999: Regional and global distributions and lifetimes of sulfate aerosols

- from Mexico City and southeast China. *J. Geophys. Res.*, **104**, 30,231-30,239.
- Bouwman, A.F., D.S. Lee, W.A.H. Asman, F.J. Dentmer, K.W. Van Der Hoek, and J.G.J. Oliver, 1997: A global high-resolution emission inventory for ammonia. *Global Biogeochem. Cycles*, **11**, 561-587.
- Chow, J.C., J.G. Watson, S.A. Edgerton, and E. Vega, 2002: Chemical composition of PM_{2.5} and PM₁₀ in Mexico City during winter 1997. *Sci. Tot. Environ.* **287**, 177-201.
- Ferm, M., 1979: Method for determination of atmospheric ammonia. *Atmos. Environ.*, **13**, 1385-1393.
- Fehsenfeld, F.C., L.G. Huey, E. Leibrock, R. Dissly, E. Williams, T.B. Reyerson, R. Norton, D.T. Sueper, and B. Hartsell, 2002: Results from an informal intercomparison of ammonia measurement techniques. *J. Geophys. Res.*, **107**, 4812-4816.
- Fraser, M.P., and G.R. Cass, 1998: Detection of excess ammonia emissions from in-use vehicles and the implications for fine particle control. *Environ. Sci. Technol.*, **32**, 1053-1057.
- Gaffney, J.S., N.A. Marley, M.M. Cunningham, and P.V. Doskey, 1999: Measurements of peroxyacyl nitrates (PANS) in Mexico City: Implications for megacity air quality impacts on regional scales. *Atmos. Environ.*, **33**, 5003-5012.
- Martin, P.A. 2002: Near-infrared diode laser spectroscopy in chemical process and environmental air monitoring. *Chem. Soc. Rev.* **31**, 201-210.
- Moeckli, M.A., M. Fierz, and M.W. Sigrist, 1996: Emission factors for ethane and ammonia from a tunnel study with a photoacoustic trace gas detection system. *Environ. Sci. Technol.*, **30**, 2864-2867.
- Pierson, W.R., and W.W. Brachaczek, 1983: Particulate matter associated with vehicles on the road. *Environ. Sci. Technol.*, **17**, 757-760.
- Schlesinger, W.H., and A.E. Hartley, 1992: A global budget for atmospheric NH₃. *Global Biogeochem. Cycles*, **15**, 191-211.
- Sutton, M.A., U. Dragositis, Y.S Tang, and D. Fowler, 2000: Ammonia emissions from non-agricultural sources in the UK. *Atmos. Environ.*, **34**, 855-869.